X-615-70-1
PREPRINT

NASA TM X-63805

OGO 4 OBSERVATIONS OF ION COMPOSITION AND TEMPERATURES IN THE TOPSIDE IONOSPHERE

S. CHANDRA
B. E. TROY, JR.
J. L. DONLEY
R. E. BOURDEAU

JANUARY 1970

GSFC
GODDARD SPACE FLIGHT CENTER
GREENBELT, MARYLAND

OGO 4 OBSERVATIONS OF ION COMPOSITION AND TEMPERATURES IN THE TOPSIDE IONOSPHERE

by

S. Chandra, B. E. Troy, Jr.,
J. L. Donley and R. E. Bourdeau
Laboratory for Space Sciences
Goddard Space Flight Center
Greenbelt, Maryland

ABSTRACT

Direct measurement of the densities of various ionic constituents (H^+, He^+, and O^+) and the temperatures of ions and electrons have been obtained from the OGO 4 planar retarding potential analyzer in the altitude range 400-900 km. Results are presented from day and night passes in the mid and low latitudes near the 1967 fall equinox. The passes are selected to emphasize the latitudinal rather than the height dependence of the measurements.

The main results can be summarized as follows:

(1) Above 800 km at night, there is a deep equatorial trough in the He^+ and a corresponding rise in O^+, suggesting a charge exchange between these two as an important loss mechanism for He^+.

(2) The dominant ion in the night at these altitudes between $\pm 40^{\circ}$ geomagnetic latitudes is H^+ followed generally by O^+ and He^+. Outside this latitude region O^+ becomes the dominant constituent increasing continuously towards the pole.

(3) The major ionic constituent in the daytime is O^+ throughout the altitude and latitude range of observations. In the height range of 400-500 km, the latitudinal variation in O^+ shows the well known feature of the geomagnetic anomaly.

(4) Both electron and ion temperatures generally increase polewards from their low latitude values. The electron temperature is measurably higher than the ion temperature even in the night time, indicating departure from thermodynamic equilibrium.

INTRODUCTION

The measurement of ion composition in the upper ionosphere started as early as 1958 with the launching of Sputnik 3 [Istomin 1961]. Soon after Nicolet [1961] suggested that helium should be considered an important constituent of the upper atmosphere, the interest in making ion composition measurements on a global scale became much more wide spread. A number of satellites and rockets have since been launched towards the fulfillment of this objective [Bourdeau et al., 1962; Bowen et al., 1964; Istomin, 1966; Hoffman, 1967; Taylor et al., 1968; Maier, 1969; Brinton et al., 1969 (a, b). See also Bauer, 1970, for other detailed references.]. More recently these efforts have been compli-mented by a network of incoherent back scatter stations [Gordon, 1967]. As a result of this intensive investigation, it is now firmly established that the main ionic constituents in the top-side ionosphere are O^+, He^+, H^+ and N^+. Their relative concen-trations depend on the altitude, latitude, local time, season and the level of solar activity. The observational data, however, is still not very extensive for the purpose of generalizing the main features of the temporal and the latitudinal changes in the ion composition. This is particularly true for the region between 400-1000 km which is very dynamic with respect to relative changes between the densities of the heavier and the lighter constituents.

One of the main objectives of OGO 4 (the fourth in the series of the orbiting geophysical observatories) was to help bridge the gap of our knowledge in this area. The satellite was launched into

a near polar orbit covering the altitude range of 400-900 km. One of the experiments aboard this satellite was a planar RPA (retarding potential analyzer) designed to measure the density and temperature of the electron and ion gas and the ion composition. The high inclination and relatively small height range of the orbit make it possible to effect some separation of the latitude and local time variations in the data. This paper presents some results on the ion composition and temperatures as measured from the RPA for late 1967, a period of moderately high solar activity.

EXPERIMENT DESCRIPTION

The experiment hardware consists of two parts: the sensor unit, located in the Orbital Plane Experiment Package (OPEP), and the electronics unit, located in the spacecraft main body. The sensor is illustrated schematically in figure 1. Three circular wire-mesh grids (G0, G1, G2) are placed in front of and parallel to a circular collector plate (C). The transparency for the three grids in combination is 0.9. All sensor elements (collector and grids) are gold-plated. The outer grid is mounted on a guard ring flush with the OPEP face; the guard ring and the OPEP are electrically isolated.

The instrument is operated alternately in an ion mode and electron mode. Appropriate voltages are applied to G2 and C so that particles of undesired charge polarity are excluded and electron photoemission from C is suppressed. A stepping voltage of 128 discrete values is applied to G1 (ion mode) or to G1 and

G0 (electron mode) to selectively retard the flow of desired particles. All voltages are with reference to spacecraft ground.

The collector is connected to an electrometer amplifier for current measurement and subsequent telemetry. At the normal spacecraft data rate, each step in the retarding voltage takes 144 milliseconds, so that one ion cycle and one electron cycle are obtained every 36.6 seconds. During accelerated data rate, the step time can be as low as 18 milliseconds.

The electrometer operates in six linear amplification ranges; the amplification changes by a factor of six from one range to the next. The maximum current which can be measured in the least sensitive range (range 6) is 5×10^{-6} amperes; the smallest measurable current in the most sensitive range (range 1) is near 10^{-12} amperes. Maximum measurable charges particle densities are on the order of $10^{6}/cm^{3}$.

During normal stabilized operation, the satellite Z-axis is maintained parallel to the satellite-earth radius vector. The OPEP is mounted on a shaft parallel to the Z-axis, and the shaft is rotated so that the normal to the OPEP face is in the orbital plane and is looking essentially along the velocity vector. The sensor is thus oriented for maximum ion collection.

DATA ANALYSIS

Data are received in the form of retarding voltage - collector current pairs, 128 pairs making up a complete curve for either the electron or the positive ion mode. Figure 2

shows a representative ion curve, and figure 3 a representative electron curve. In order to stretch out the horizontal scale and thus show the significant portions of the curves in more detail, the ion plateau current at retarding voltage $\leq$ 2.0 V and the electron background current at retarding voltage < 1.0 V are not shown.

Although some information about the density and temperature can be obtained quickly from the measurement of the plateau current and the slope of the current voltage (I-V) curves, we rely chiefly on data processing by computer to analyze large numbers of curves and determine all densities and temperatures in final form. A curvefitting technique based on the principle of minimum variance is used in which density, temperature and spacecraft potential are varied until the resulting calculated I-V curve attains a highly accurate fit with the actual data. The fits so obtained for the data in figures 2 and 3 are shown as solid lines. A complete description of the technique has been published earlier [Moss and Hyman, 1968].

After the experimental data from several passes had been analyzed, it was seen that the program could consistently separate helium from hydrogen, but not nitrogen from oxygen. Results from other experiments indicate that $n(N^+) \ll n(O^+)$ in the OGO 4 region of measurement [Hoffman, 1967; Taylor et al., 1968]. Under this assumption, further tests were made with both theoretically generated data and experimental data; these tests showed that our results were not changed significantly by leaving nitrogen off the list of ionic components. Consequently, density

measurements presented in this paper will include only hydrogen, helium and oxygen. It should also be noted that all ionic components are assumed to have the same temperature T_+.

During the periods covered by this paper, ϕ_s remains more negative than -2 V; in fact, ϕ_s makes frequent excursions beyond -7 V when the satellite is in the sun. Whipple and Parker [1969] have shown that conventional analysis of electron I-V curves taken on a negative satellite will yield correct electron temperature T_e, but incorrect values of ϕ_s (>true ϕ_s) and electron density n_e (< true n_e). We have often seen periods when ou results give

$$\phi_s(\text{electron}) > \phi_s \text{ (ion)}$$

and

$$n_e < n_+$$

Because Whipple and Parker's work seems to explain these results, and because we believe that n_+ determined by the ion plateau current is more accurate than n_e determined by the "break point" in the electron curve, we delete n_e from our results presented here.

The highly negative satellite potential experienced in the day also has an undesirable effect on the ion analysis. Under such a condition, very little or none of the retarded portion of the ion curve will be recorded. It is then impossible to determine T_+, although n_+ may be obtained from the plateau current value.

In the high latitude regions there are considerable temporal and/or spatial variations in the ionosphere. Consequently, ionospheric conditions may change a great deal during the time necessary to record one I-V curve (18 sec. for the normal data rate). Under these conditions, the analysis technique, which assumes constant conditions, cannot properly fit the curve. Our results in this paper are therefore limited to low and middle latitudes, except where we compute ion density directly from the plateau current.

EXPERIMENTAL RESULTS

For the polar orbiting OGO 4, the local time of the satellite remains essentially constant during a single north-south or south-north pass (polar areas excepted). Therefore, variations in the measured ion composition and temperature during one such pass are due to changes in altitude and latitude. In order to emphasize the latitudinal dependence of the results presented here, we restrict ourselves to periods when the apogee and perigee are relatively close to the equator. The periods are: (1) September, 1967, with a night apogee and a day perigee, and (2) late October 1967, when the orbital precession resulted in a day apogee and a night perigee.

Figure 4 shows a representative night time apogee pass for the equinox condition. Plotted here are the O^+, He^+ and H^+ densities along with the electron and ion temperatures. The measured parameters in this figure, and in the remaining figures in this paper, are plotted versus geomagnetic latitude. As

discussed earlier, the retarding potential technique does not permit the resolution of both N^+ and O^+ with sufficient accuracy. Accordingly, the latitudinal variation in O^+ shown here may also be interpreted as the variation of the sum of O^+ and N^+, even though the latter may constitute only a small percentage of the sum. We shall return to this point later in the paper when discussing the physical significance of these variations.

The latitudinal variations in electron temperature are very similar to the ones observed in the 1000 km range from Exlorer 22, i.e, increasing from the equator towards the poles, first gradually and then rather rapidly after the latitude region of $\pm$ 40° [Brace et. al., 1967]. The ion temperature follows a similar pattern, though it is consistently lower than the electron temperature by at least 200° K, indicating that thermal equilibrium has not been reached between the electron and ion gas in the night time.

The latitudinal variation in the ion composition is quite complex. In the equatorial region ($\pm$ 20° geomagnetic latitude), H^+ is the major constituent, followed by O^+ and He^+. The relative concentration of these constituents change quite drastically with latitude, suggesting a complex pattern of change in transition height with latitude. Both He^+ and O^+ increase towards the poles, though He^+ increases much more rapidly than O^+. In the mid-latitude region, it is difficult to make a definite statement about the relative concentration of these ions. In the particular

pass shown here, H^+ continues to be the major ion followed by He^+ and O^+ in the northern hemisphere. In the southern hemisphere, this order is altered beyond -30^o geomagnetic latitude where He^+ becomes the dominant constituent followed by O^+ and H^+. In interpreting these differences, it is important to consider the altitude variations of the spacecraft over a given pass. This effect is most strongly manifested in O^+ and least in H^+ owing to the difference in their scale heights.

The most remarkable feature of the night time composition is the presence of a deep trough in He^+ in the equatorial region. In almost all the passes studied so far, the depletion in He^+ is accompanied by an enhancement in O^+. This point is substantiated in Figure 5, which shows the latitudinal variations in the ionic constituents for three different apogee passes through the equator. The latitudinal position of the apogee is indicated by a vertical line. The local time at the equator for each of these passes is about 0120. The anticorrelation between O^+ and He^+ near the equator is quite evident in all three passes, with H^+ being dominant followed by O^+ and He^+. In the midlatitudes, H^+ usually continues to be the major ion, followed by He^+ and O^+. There are few exceptions to this generalization, which are probably associated with the altitude variation of the satellite.

Figure 6 shows a daytime apogee pass, illustrating the latitudinal variations of electron temperature and O^+ density in the 800-900 km. altitude range. The large negative satellite

potentials experienced during the day preclude determining ion temperature, as mentioned earlier.

Since the altitude variation on this pass is almost symmetrical with respect to the geomagnetic equator, the latitudinal variations in O^+ and T_e can be attributed to solar and geomagnetic effects as indicated by the changes in solar zenith angle and geomagnetic latitude. The geomagnetic anomaly, which is quite persistent in the daytime below 500 km (Figure 7) is absent above 800 km. The O^+ density, which is one or two orderds of magnitude greater than its night time value, develops a bulge in the southern hemisphere, indicating control by the solar zenith angle. This control of the electron density and ion composition at this altitude is a well-studied feature of the topside region [Chandra and Rangaswamy, 1967; Brinton et al, 1969(b)].

Since the ion curves were not analyzed by the minimum variance technique, the H^+ and He^+ densities are not available for this pass. However, visual inspection of the mid and low latitude ion curves showed that the collected current due to the light components (see Figure 2) was about the same order of magnitude as at night, although the total current due to all components was an order of magnitude greater than at night. We can therefore infer that the sum of the densities of H^+ and He^+ between 800 and 900 km does not change drastically from local time 0130 to local time 0930.

The electron temperature on this pass exhibits a strong latitudinal variation. Both the gradients and the absolute values are higher here than at night. An interesting feature of the T_e profile is the existence of the maxima at about 40^o - 50^o geomagnetic latitude on either side of the equator. The presence of these maxima appear to be a very stable feature in the latitudinal variation of T_e [Brace et. al., 1967].

The temperatures and ion density below 500 km are shown in Figure 7 and 8, corresponding to midafternoon and early night passes. Again, the daytime results are without ion temperature due to the high negative satellite potential. There is no evidence of H^+ or He^+ on these passes, meaning that their densities must be less than 5% of the O^+ density.

The formation of the daytime geomagnetic anomaly (Figure 7) is quite evident. The corresponding latitudinal variation in T_e exhibits an interesting pattern in maintaining an inverse relation with the ion density throughout the latitude region. The formation of the temperature troughs near the density peaks is very suggestive. We are not certain at this stage if this is a regular feature of the electron temperature distribution in the low altitude range of the F-region. It will be necessary to study a large number of passes before a definite statement can be made about the permanence of this inverse relation in the anomaly region.

In the early night pass shown in Figure 8, the anomaly is

present in the density profile, although not as strikingly as in the day. This observation is consistent with previous reports that the anomaly becomes less pronounced early in the night and then disappears after midnight [Eccles and King, 1969]. The ion density in the equatorial region is quite comparable to its daytime values, consistent with the well known feature of post sunset density increase in this region. The asymmetry in the ion density variation with respect to the geomagnetic equator may partly be attributed to the asymmetry in the solar zenith angle.

The temperature behavior here is similar to that at night near apogee, i.e. increasing strongly poleward beyond $\pm$ 40^{o} geomagnetic latitude (see Figure 4). The departure from thero-dynamic equilibrium is maintained throughout the latitude region, with T_e being consistently higher than T_+. A small but noticeable difference between the temperature profiles of Figure 4 and Figure 8 is the broad maximum in the equatorial (anomaly) region of Figure 8, seen most easily in the T_+ profile.

SUMMARY OF THE EXPERIMENTAL RESULTS

In the previous section we have presented ion composition and temperature and electron temperatures in the topside ionosphere for selected conditions. The main features we find are as follows:

1. Above 800 km at night H^+ is generally the dominant ion below 40^{o} geomagnetic latitude. There is a strong inverse relation

between $n(O^+)$ and $n(He^+)$ near the equator. Somewhere beyond 40^o latitude, O^+ becomes the major ion while $n(H^+)$ and $n(He^+)$ decrease. Both T_+ and T_e show sharp increases toward the poles from relatively constant lower latitude values.

(2) During midmorning in the same altitude range, $n(O^+)$ has increased from its values at night so that O^+ dominates at all latitudes. There is some indication that the densities of the light ions remain roughly the same. A peak in T_e is seen in each hemisphere.

(3) Below 500 km, O^+ is the only ion detected by the RPA. The variation of $n(O^+)$ with latitude shows the geomagnetic anomaly until at least 2124 in the evening. Ion and electron temperatures increase toward the pole, as they do at higher altitude. There is a slight rise in temperature in the anomaly region at night.

DISCUSSION

In the topside region, the major processes controlling the particle and temperature distributions are diffusion and heat conduction. These processes, in turn, are strongly controlled by the earth's magnetic field. Colin et.al., [1969], using the concept of diffusive equilibrium along field lines, have derived the ionic distribution at 1000 km in the mid-latitude region. In spite of the many simplifying assumptions made in their derivation, the general nature of the distributions of H^+, He^+ and O^+ are in very good agreement with the observations of OGO 4.

In the night equatorial region, the relative variations of O^+ and He^+ present a complex situation. The rapid increase of He^+ and the corresponding decrease in O^+ (Figs. 4 and 5) cannot be attributed to simple diffusion mechanism. In fact, the inverse relation between He^+ and O^+ suggests the possibility that the latter is being formed at the expense of the former. The chemical processes giving rise to this situation are the following [Bates and Patterson, 1961; Dalgarno, 1964; Bauer, 1966; Maier, 1968]

$$He^+ + N_2 \rightarrow N^+ + N + He \qquad (1)$$

$$He^+ + O_2 \rightarrow O^+ + O + He \qquad (2)$$

$$He^+ + O \rightarrow O^+ + He \qquad (3)$$

All three reactions involve charge transfer. The first two are disscoiative and the third one is radiative in nature. Since in these reactions O^+ or N^+ are being created at the expense of He^+, it would seem that any one or all of them could be consistent with the observations of OGO 4. As pointed out earlier, the bulge in O^+ in the equatorial region may very well correspond to the enhancement in N^+ since the RPA sensor aboard OGO 4 cannot resolve the mass differences between 14 and 16 a.m.u. with sufficient accuracy. However, it seems more likely that the radiative charge transfer between He^+ and O is an effective loss process in the altitude range of 800 km. Very little is known about the reaction rate of this process. It is probably two

orders of magnitude less than the reaction rates corresponding to the process 1 and 2, which are in the range of 10^{-9} -- 10^{-10} cm^3/sec. However, this is more than compensated by the differences in the relative concentrations of 0, N_2 and 0_2. In the altitude range of 800 km, atomic oxygen dominates over molecular oxygen and nitrogen by several orders of magnitude.

It must be emphasized here that the charge transfer between He^+ and 0 as a means of removing He^+ from the atmosphere is inferred only from a limited amount of observational data drom OGO 4. This mechanism, if important, has a great potentiality in resolving some of the problems of the helium budget in the atmosphere. A more comprehensive analysis of OGO 4 data is in progress to establish the consistency of these observations over a longer period and to estimate the reaction rate for this process.

GEOMAGNETIC ANOMALY

As shown in Figures 7 and 8, the most striking feature of the latitudinal variations below 500 km is the existence of maxima in the 0^+ distribution at about 20^o latitude on either side of the equator. This phenomenon, generally known as the geomagnetic anomaly, is one of the most widely discussed topic in the literature [See for example Cohen 1967, Goldberg 1969], and is another example of diffusion as a controlling process in the topside region of the ionosphere. The physical basis of the formation of the geomagnetic anomaly is easy to comprehend

in terms of the geometrical properties of the earth's magnetic and gravitational fields. This is illustrated in Figure 9, by a two dimensional representation of the plasma distribution in the earth's dipole field. The magnetic field lines are illustrated by white lines,and altitudes with respect to the surface are indicated by the parallel concentric lines (both broken and white). The electron (or ion) density distribution in this configuration is shown by the variations in the background shades. The region of the darkest shade in this illustration corresponds to the region of the highest density and the region of the lightest shade corresponds to the region of the lowest density. The physical basis of this illustration is as follows: assume that the vertical density distribution at the equator is parabolic or Chapman-like, with a peak at about 500 km (illustrated in the lower portion of the Figure 9). Based on the concept of field-aligned diffusive equilibrium, the density distribution along any field line will depend upon the density of the region through which this field line passes at the equator. Thus, a field line passing through the region of maximum ionization at the equator will have maximum density along its path. The field lines passing through the equator above and below the height of the maximum density accordingly will reflect the region of lower densities. The density along any field line, of course, is not constant. Along its path it decreases slowly, depending upon the plasma scale height and the change in altitude.

In such a configuration, an observer crossing the latitudes at fixed heights will encounter density variations very similar to the one shown in the lower portion of Figure 9 by the dashed curve. Moving away from the equator, the electron or ion density slowly increases, becomes maximum in the 10-15^{o} latitude zone and falls off towards the poles. The mathematical basis for this illustration has been discussed by Chandra and Goldberg [1964]. The simple picture presented here is meant to emphasize that the geomagnetic anomaly is a very natural configuration of an ionospheric plasma in an equilibrium state, under the influence of the geomagnetic and graviatational fields. There is no implication that processes like production, loss and transport do not play any role in the formation of the equatorial F-region. The effect of these processes have been discussed extensively in the literature [Bramley and Peart, 1965; Kendall and Windle, 1965; Windle and Kendall, 1965; Hanson and Moffett, 1966] and must be considered in making a detailed comparison of the observational data with the theoretical predictions.

Another example of the influence of the magnetic field in the topside F-region is latitudinal increase in electron and ion temperature as discussed in the previous section. The electron temperature measurements from IMP-2 [Serbu and Maier, 1966] have revealed that electron temperature in the equatorial region above 1.5 earth radii increases directly as the square of the radial distance. Based on the concept of field-aligned heat conduction for the charged particles, this observation is

consistent with the increase in electron temperature towards higher latitudes as measured from OGO 4. The source of the energy for this increase is probably the auroral region itself, where the flux of energetic electrons is substantially increased [Maier and Rao, 1969].

CONCLUSION

In this paper we have presented results on the latitudinal variations in ion composition and temperature in the topside region for the equinox or near equinox conditions. The most interesting result is the inverse relation between the O^+ and He^+ variations in the night time equatorial region above 800 km. These observations give the first indication of the radiative charge transfer between He^+ and O as a mechanism for the destruction of helium ions. The latitudinal variations in density and temperature show strong influence of the solar zenith angle and the earth's geomagnetic field.

The simultaneous measurements of electron and ion temperature give us the indication that the electron and ion gas below 900 km are not in thermodynamic equilibrium even in the night time.

ACKNOWLEDGEMENT

The authors would like to express their appreciation to Dr. S. J. Bauer for many helpful discussions.

REFERENCES

Bates, D.R., and T.N.L. Patterson, Hydrogen atoms and ions in the thermosphere and exosphere, Planetary Space Sci., 5, 257, 1961.

Bauer, S.J., Chemical processes involving helium ions and the behavior of atomic nitrogen ions in the upper atmosphere, J. Geophys. Res., 71, 1508, 1966.

Bauer, S.J., Rocket and satellite experiments in the magnetospnere, Handbuch d. Physik, 49, Geophys.IV/4, 1970.

Bourdeau, R.E., E.C. Whipple, Jr., J.L. Donley, and S.J. Bauer, Experimental evidence for the presence of helium ions based on Explorer VIII satellite data, J. Geophys. Res., 67, 467, 1962.

Bowen, P.J., R.L.F. Boyd, W.J. Raitt, and A.P. Willmore, Ion composition of the upper F-region, Proc. Royal Soc., 281, 504, 1964.

Brace, L.H., B.M. Reddy, and H.G. Mayr, Globel behavior of the ionosphere at 1000-kilometer altitude, J. Geophys. Res., 72, 265, 1967.

Bramley, E.N., and M. Peart, Diffusion and electromagnetic drift in the equatorial F2 region, J. Atmospheric Terrest. Phys., 27, 1201, 1965.

Brinton, H.C., M.W. Pharo, III, H.G. Mayr, and H.A. Taylor, Jr., Implications for ionospheric chemistry and dynamics of a direct measurement of ion composition in the F_2 region, J. Geophys. Res., 74, 2941, 1969(a).

Brinton, H.C., R.A. Pickett, and H.A. Taylor, Jr., Diurnal and seasonal variations of atmospheric ion composition; correlation with solar zenith angle, J. Geophys. Res., 74, 4064, 1969(b).

Chandra, S., and R.A. Goldberg, Geomagnetic control of diffusion in the upper atmosphere, J. Geophys. Res., 69, 3187, 1964.

Chandra, S., and S. Rangaswamy, Geomagnetic and solar control of ionization at 1000 km., J. Atmospheric Terrest. Phys., 29, 259, 1967.

Cohen, R., The equatorial ionosphere, in Physics of Geomagnetic Phenomena, edited by S. Matsushita and W. Campbell, p. 561, Academic Press, New York, 1967.

Colin, L., S.W. Dufour, and D.S. Willoughby, An interpretation of OGO light ion abundance measurements, J. Geophys. Res., 74, 1863, 1969.

Dalgarno, A., Thermal reactions involving charged particles, Discussions of the Faraday Society, 37, 142, 1964.

Eccles, D., and J.W. King, A review of the topside sounder studies of the equatorial ionosphere, Proc. IEEE, 57, 1012, 1969.

Goldberg, R.A., A review of the theories concerning the equatorial F2 region ionosphere, Proc. IEEE, 57, 1119, 1969.

Gordon, W.E., F region and magnetosphere backscatter results, Reviews of Geophysics, 5, 191, 1967.

Hanson, W.B., and R.J. Moffett, Ionization transport effects in the equatorial F region, J. Geophys. Res., 71, 5559, 1966.

Hoffman, J.H., Composition measurements of the topside ionosphere, Science, 155, 322, 1967.

Istomin, V.G., Variation in the positive ion concentration with altitude from data of mass spectrometry measurements on the third satellite, Planetary Space Sci., 8, 179, 1961.

Istomin, V.G., Observational results on atmospheric ions in the region of the outer ionosphere, Ann. Geophys., 22, 255, 1966.

Kendall, P.C., and D.W. Windle, A possible explanation of the Appleton anomaly of the F2 layer; Dougherty's theory of ion drag, J. Atmospheric Terrest. Phys., 27, 795, 1965.

Maier, E.J.R., Sounding rocket measurements of ion composition and charged particle temperatures in the topside ionosphere, J. Geophys. Res., 74, 815, 1969.

Maier, E.J., and B.C. Narasinga Rao, Observations of the suprathermal electron flux and the electron temperature at high latitudes, paper presented at the fall URSI meeting, Austin, Texas, 1969.

Maier, W.B., II, Reactions of He^+ with N_2 and O_2 in the upper atmosphere, Planetary Space Sci., 16, 477, 1968.

Moss, S.J., and E. Hyman, Minimum variance technique for the analysis of ionospheric data acquired in satellite retarding potential analyzer experiments, J. Geophys. Res., 73, 4315, 1968.

Nicolet, M., Helium, an important constituent in the lower exosphere, J. Geophys. Res., 66, 2263, 1961.

Serbu, G.P., and E.J.R. Maier, Low-energy electrons measured on IMP 2, J. Geophys. Res., 71, 3755, 1966.

Taylor, H.A., Jr., H.C. Brinton, M.W. Pharo, III, and N.K. Rahman, Thermal ions in the exosphere; evidence of solar and geomagnetic control, J. Geophys. Res., 73, 5521, 1968.

Whipple, E.C., Jr., and L.W. Parker, Theory of an electron trap on a charged spacecraft, J. Geophys. Res., 74, 2692, 1969.

Windle, D.W. and P.C. Kendall, A possible explanation of the Appleton anomaly of the F2 layer II. A model with unequal horizontal velocities, J. Atmospheric Terest. Phys., 27, 1163, 1965.

FIGURE CAPTIONS

Figure 1 - Schematic of RPA sensor.

Figure 2 - Ion current-voltage curve with minimum variance fit.

Figure 3 - Electron current-voltage curve with minimum variance fit.

Figure 4 - The latitudinal variations in electron and ion temperatures and ion composition for a night time apogee pass through the equator. The temperatures and ion densities are plotted against the running scales of the altitude, solar zenith angle and geomagnetic latitude.

Figure 5 - The latitudinal variations in ion composition showing the equatorial trough in He^+. The positions of the apogee are marked by vertical lines.

Figure 6 - The latitudinal variations in electron temperature and O^+ density for a daytime apogee pass through the equator. The temperature and ion density are plotted against the running scales of altitude, solar zenith angle and geomagnetic latitude.

Figure 7 - Electron temperature and O^+ density for a daytime perigee pass through the equator. The changes in altitude, solar zenith angle and geomagnetic latitude are shown by means of the three running scales.

Figure 8 - The latitudinal variations in electron and ion temperatures and O^+ density for a night time perigee pass through the equator. The three running scales show

Figure 8 - the changes in altitude, solar zenith angle and (Cont')
the geomagnetic latitude.

Figure 9 - The schematic showing the basic principles of the geomagnetic anomaly.

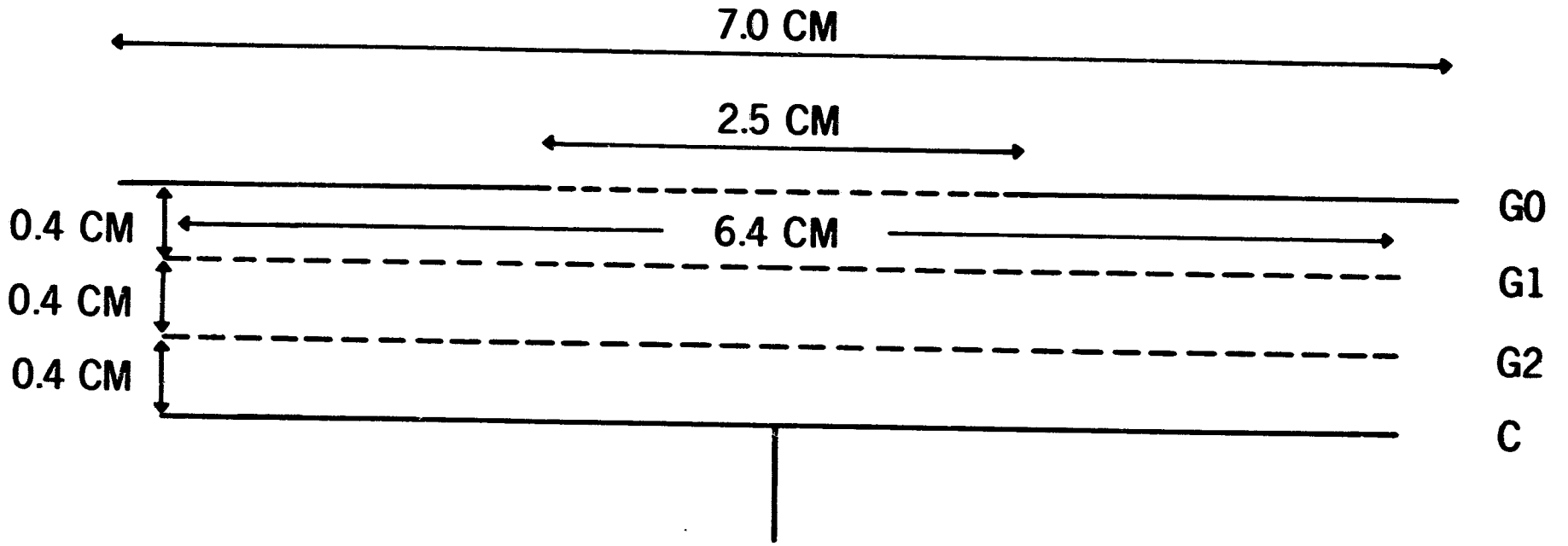

	ION MODE	ELECTRON MODE
G0	0 V	−3.2 V TO +7.0 V
G1	+12.6 V TO −0.1 V	
G2	−17 V	+10 V
G3	−2 V	+25 V

Figure 1 - Schematic of RPA sensor

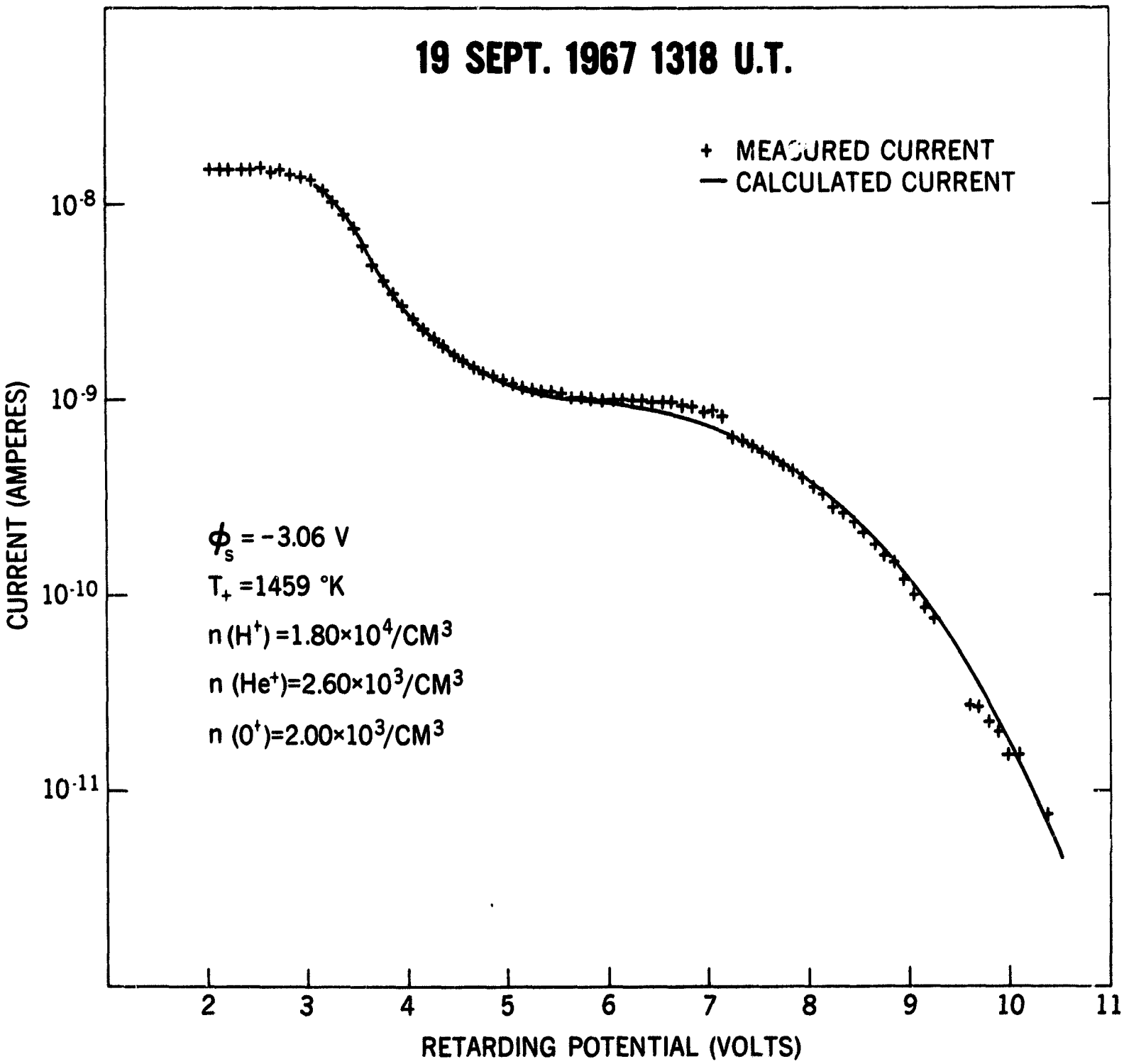

Figure 2 - Ion current-voltage curve with minimum variance fit

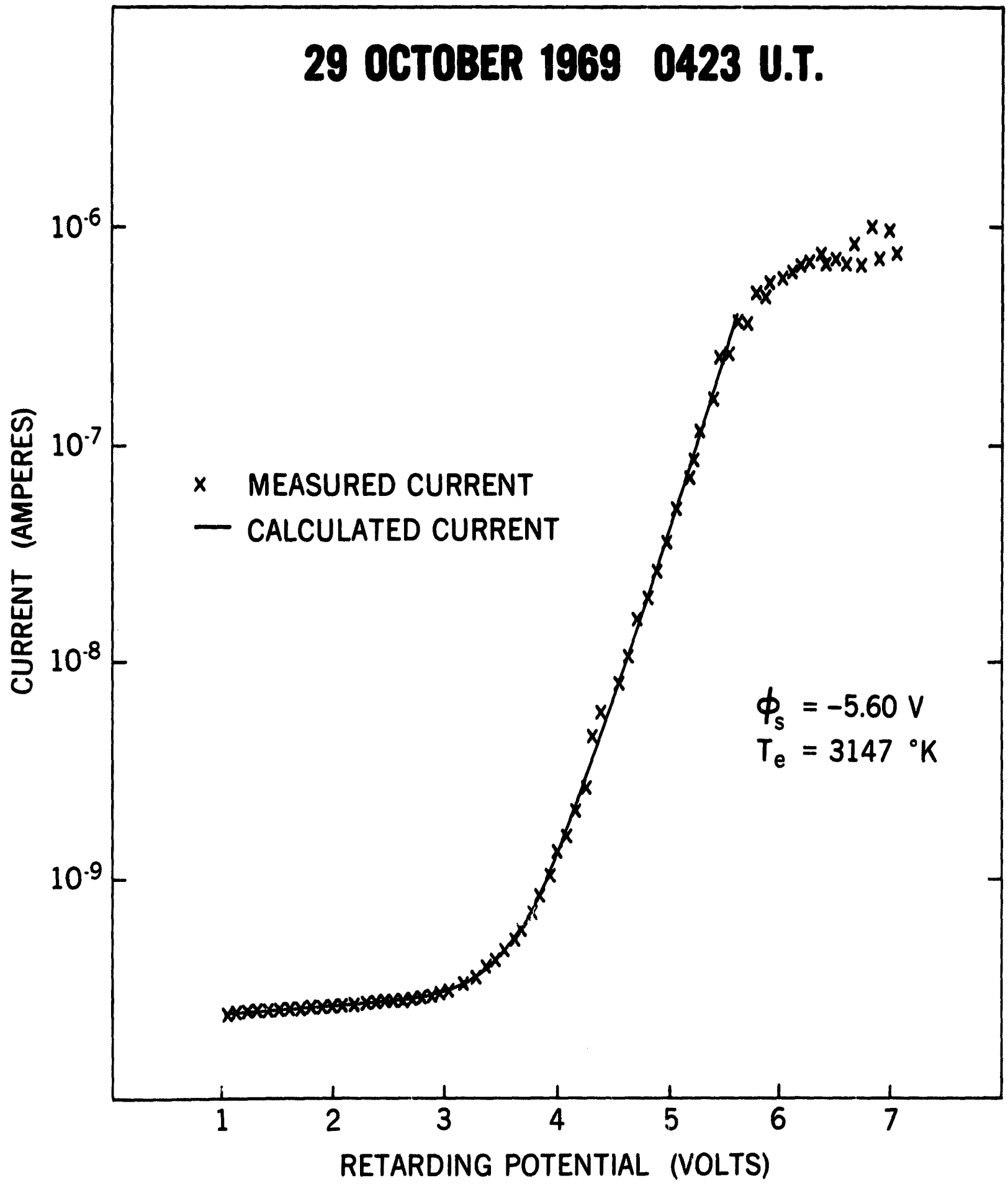

Figure 3 - Electron current-voltage curve with minimum variance fit.

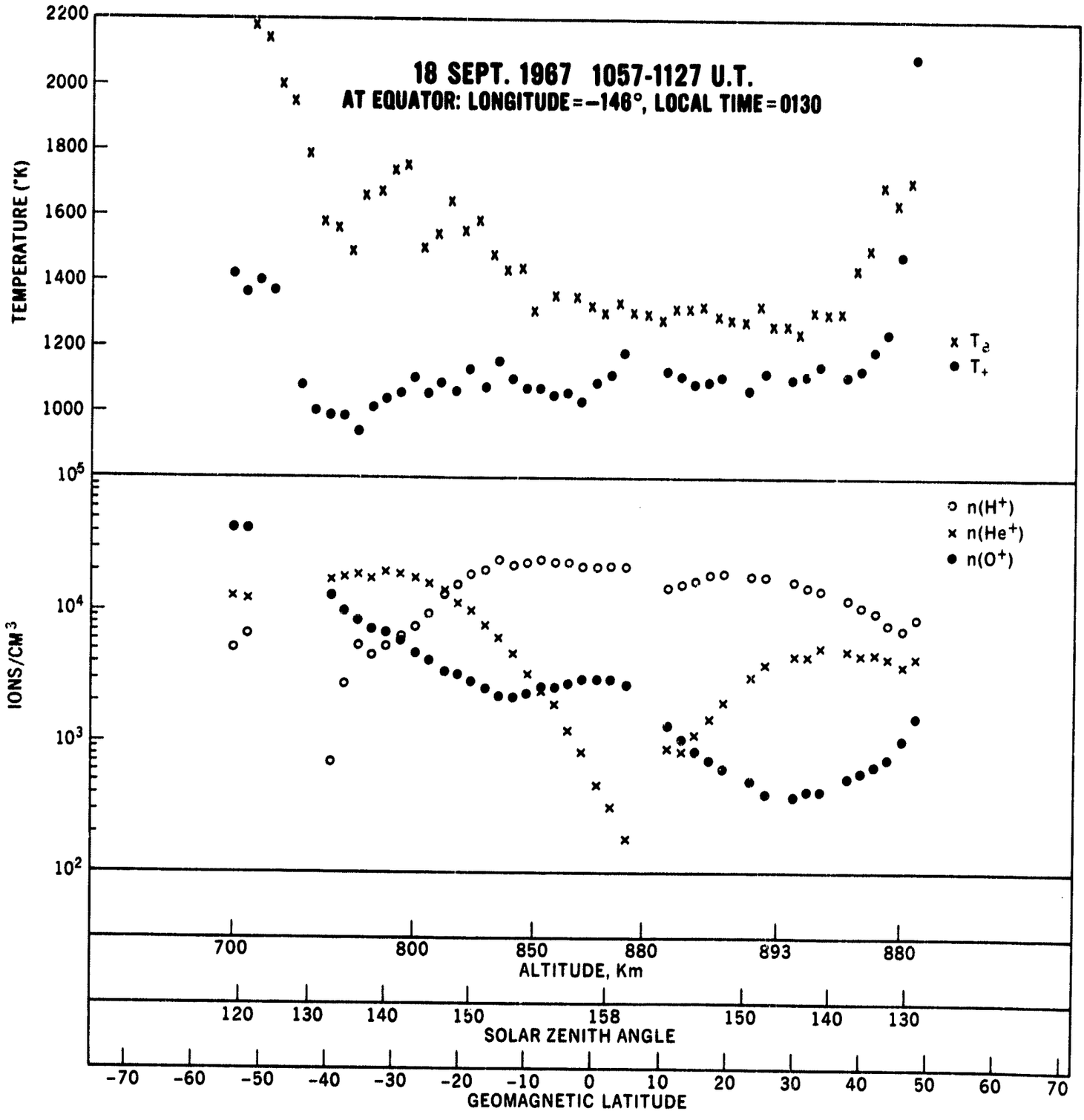

Figure 4 - The latitudinal variations in electron and ion temperatures and ion composition for a night time apogee pass through the equator. The temperatures and ion densities are plotted against the running scales of the altitude, solar zenith angle and geomagnetic latitude.

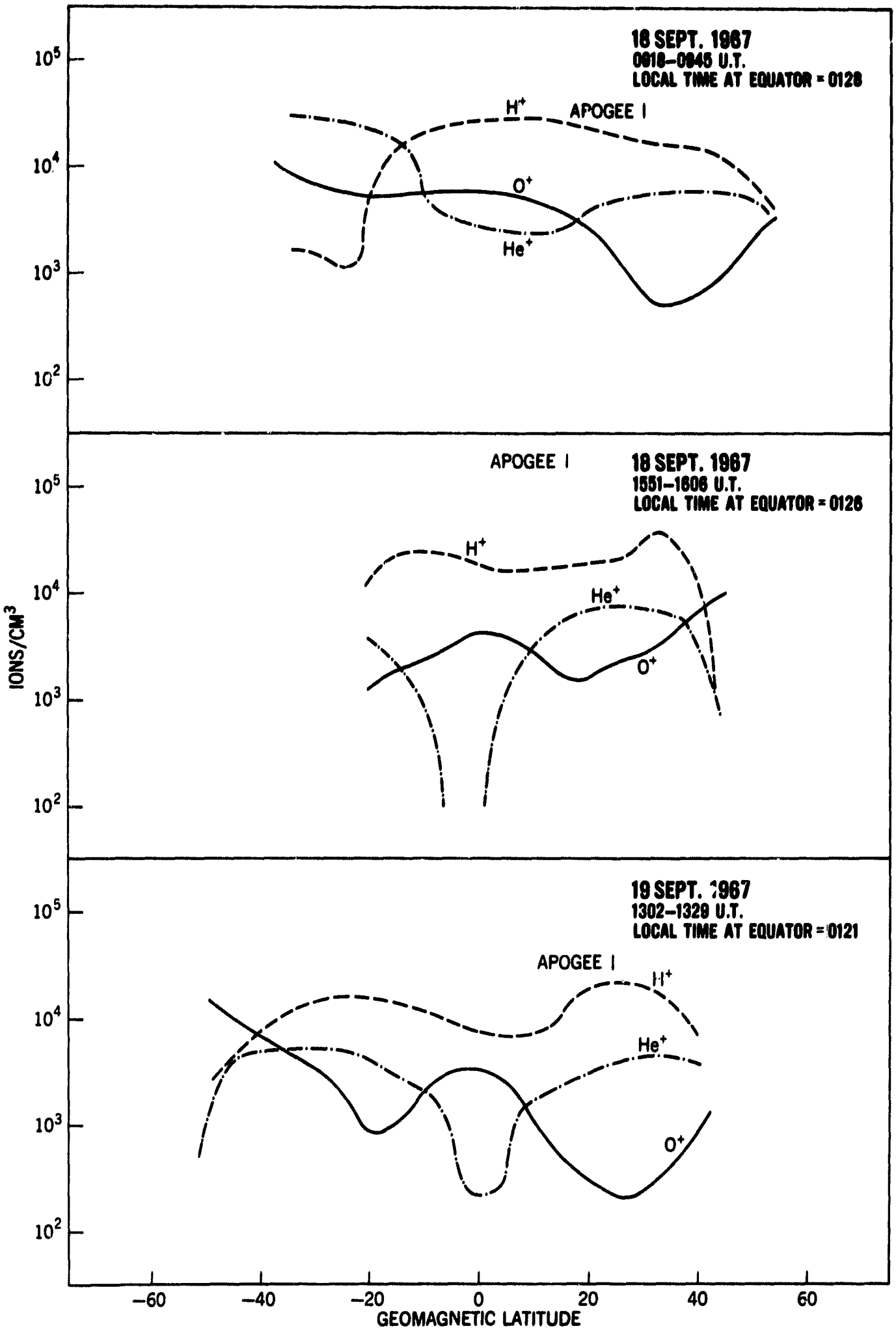

Figure 5 - The latitudinal variations in ion composition showing the equatorial trough in He^+. The positions of the apogee are marked by vertical lines.

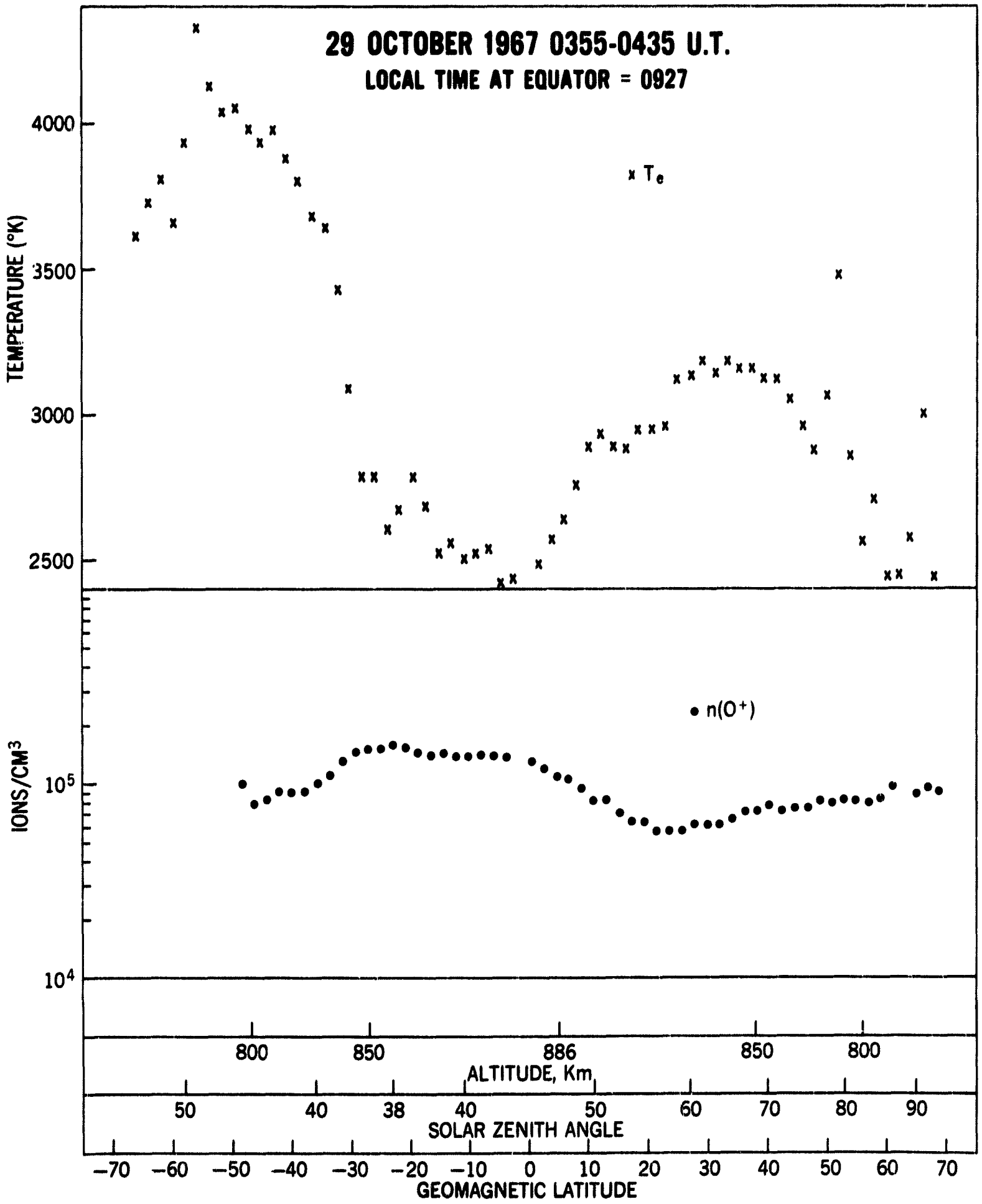

Figure 6 - The latitudinal variations in electron temperature and O^+ density for a daytime apogee pass through the equator. The temperature and ion density are plotted against the running scales of altitude, solar zenith angle and geomagnetic latitude.

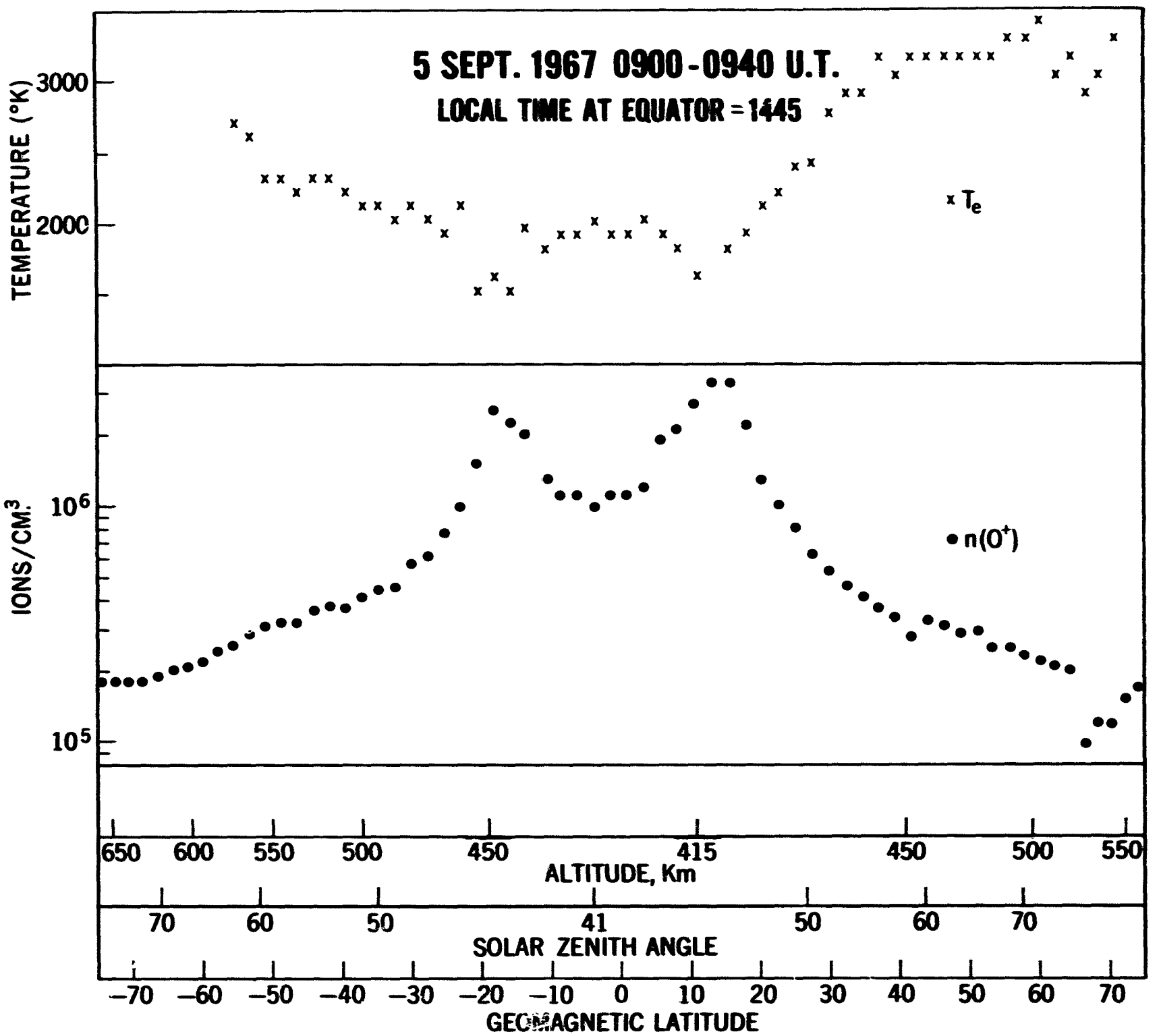

Figure 7 - Electron temperature and O^+ density for a daytime perigee pass through the equator. The changes in altitude, solar zenith angle and geomagnetic latitude are shown by means of the three running scales.

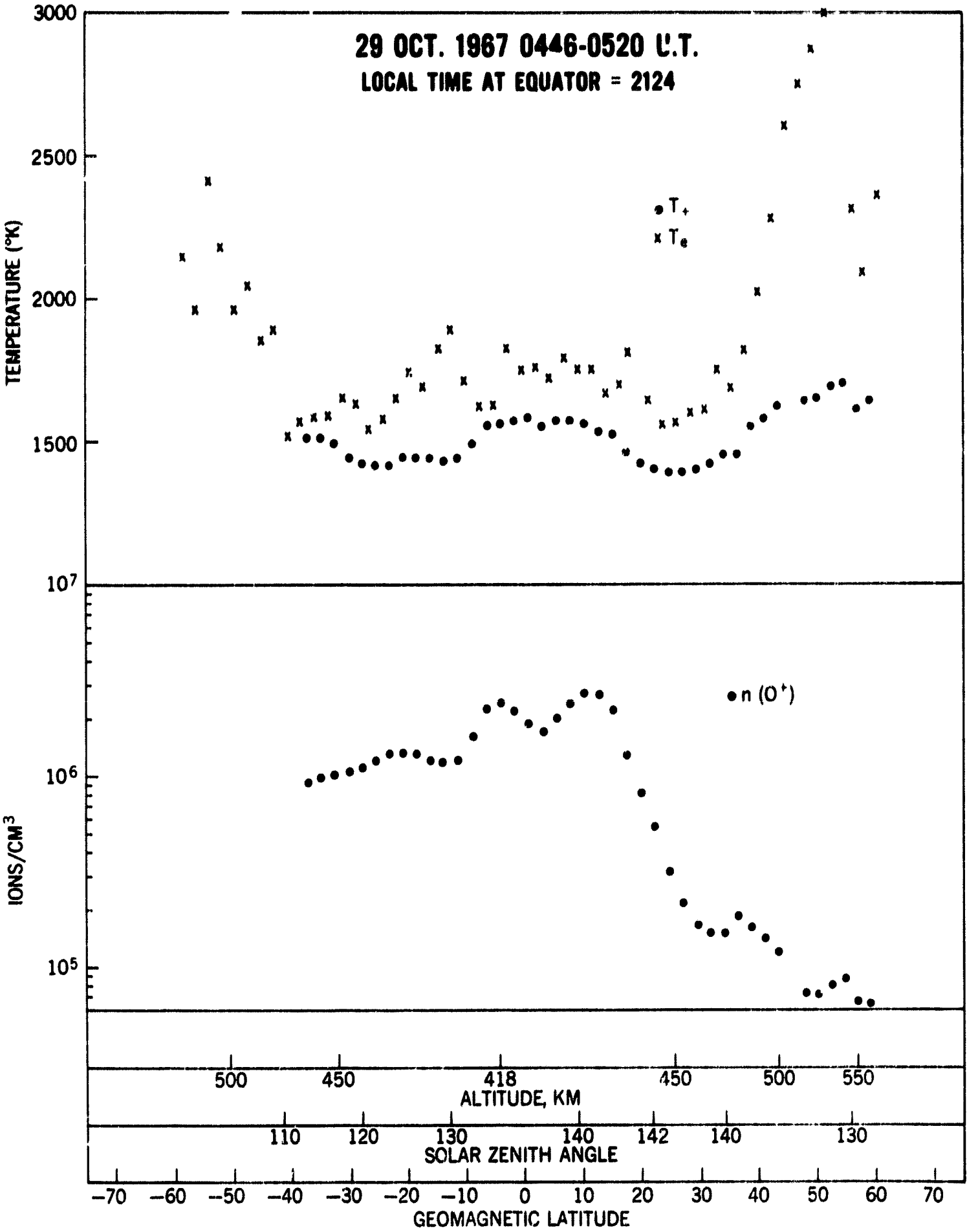

Figure 8 - The latitudinal variations in electron and ion temperatures and O^+ density for a night time perigee pass through the equator. The three running scales show the changes in altitude, solar zenith angle and the geomagnetic anomaloy.

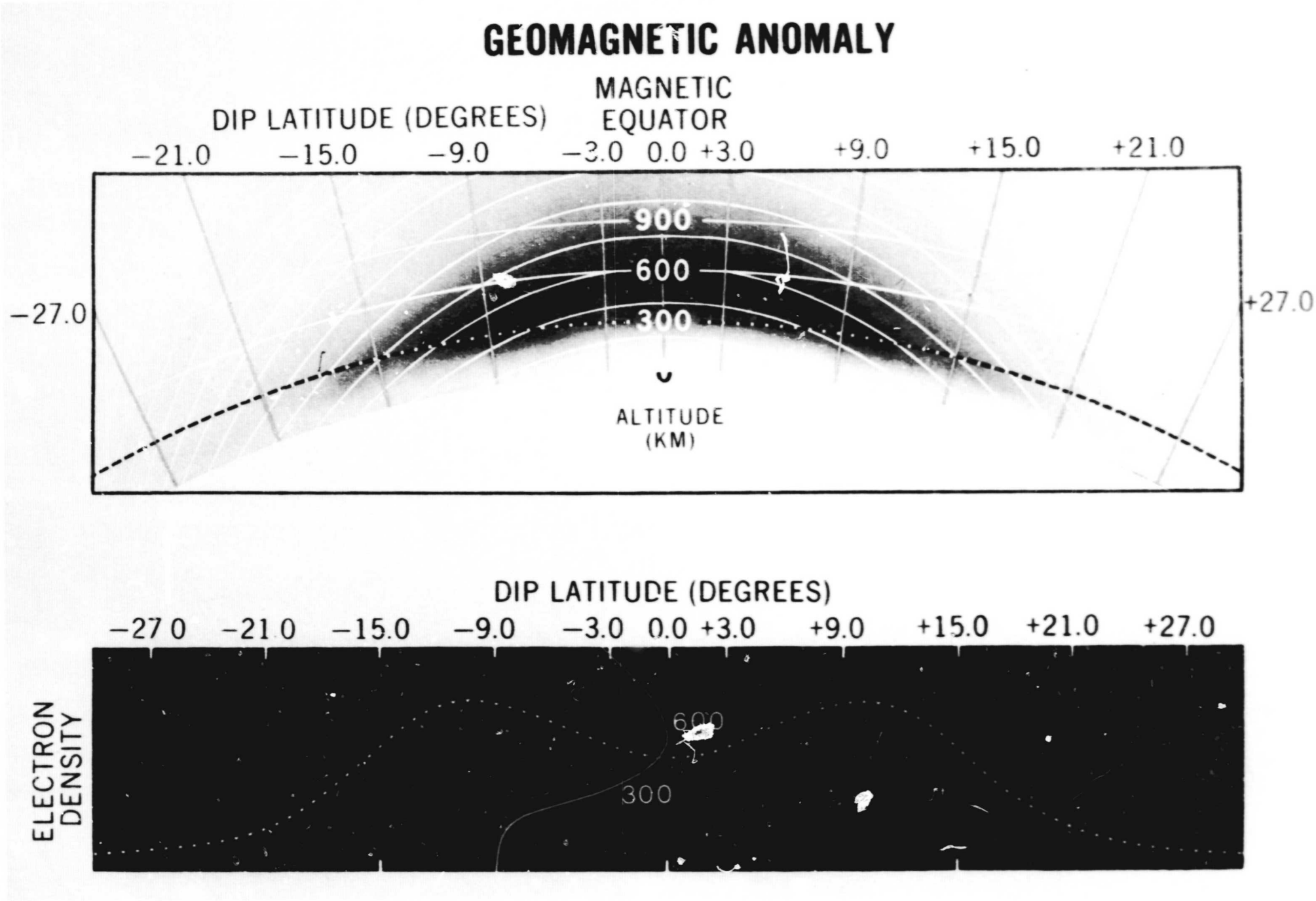

Figure 9 - The schematic showing the basic principles of the geomagnetic anomaly.